

**Jānis Narbutis**

**ADAPTIVE BUILDING FACADE SYSTEMS WITH  
THERMAL ENERGY STORAGE**

Summary of the Doctoral Thesis



**RIGA TECHNICAL UNIVERSITY**

Faculty of Natural Sciences and Technology  
Institute of Energy Systems and Environment

**Jānis Narbutis**

Doctoral Student of the Study Programme “Environmental Engineering”

**ADAPTIVE BUILDING FACADE SYSTEMS  
WITH THERMAL ENERGY STORAGE**

**Summary of the Doctoral Thesis**

Scientific supervisors

Professor Dr. sc. ing.  
RUTA VANAGA

Tenured Professor Dr. sc. ing.  
ANDRA BLUMBERGA

RTU Press  
Riga 2026

Narbutis, J. Adaptive Building Facade Systems with Thermal Energy Storage. Summary of the Doctoral Thesis. Riga: RTU Press, 2026. – 42 p.

Published in accordance with the decision of the Promotion Council “RTU P-19” of 12 March 2026, No. 240.

This Thesis research has been supported by the European Social Fund within the Project No. 8.2.2.0/20/I/008 “Strengthening of PhD students and academic personnel of Riga Technical University and BA School of Business and Finance in the strategic fields of specialization” of the Specific Objective 8.2.2 “To Strengthen Academic Staff of Higher Education Institutions in Strategic Specialization Areas” of the Operational Programme “Growth and Employment”.

NACIONĀLAIS  
ATTĪSTĪBAS  
PLĀNS 2020



EIROPAS SAVIENĪBA

Eiropas Sociālais  
fonds



**FLPP**

FUNDAMENTAL AND  
APPLIED RESEARCH  
PROJECTS

---

I E G U L D Ī J U M S T A V Ā N Ā K O T N Ē

Cover image by Jānis Narbutis.

<https://doi.org/10.7250/9789934373077>

ISBN 978-9934-37-307-7 (pdf)

# **DOCTORAL THESIS PROPOSED TO RIGA TECHNICAL UNIVERSITY FOR PROMOTION TO THE SCIENTIFIC DEGREE OF DOCTOR OF SCIENCE**

To be granted the scientific degree of Doctor of Science (PhD), the present Doctoral Thesis has been submitted for defence at the open meeting of RTU Promotion Council on 11 June 2026, at 14.00 at the Faculty of Natural Sciences and Technology, Āzenes iela 12, k/1, Room 607.

## **OFFICIAL REVIEWERS**

Associate Professor Vladimirs Kirsanovs  
Riga Technical University

Professor Dr. sc. Peter D. Lund  
Aalto University, Finland

PhD Jurgis Zagorskas  
Vilnius Gediminas Technical University, Lithuania

## **DECLARATION OF ACADEMIC INTEGRITY**

I hereby declare that the Doctoral Thesis submitted for review to Riga Technical University for promotion to the scientific degree of Doctor of Science (PhD) is my own. I confirm that this Doctoral Thesis has not been submitted to any other university for promotion to a scientific degree.

Jānis Narbutis ..... (signature)

Date: .....

The Doctoral Thesis has been written in English. It consists of an Introduction, 6 chapters, Conclusions, 127 figures, and 37 tables; the total number of pages is 311. The Bibliography contains 195 titles.

# TABLE OF CONTENTS

|   |    |
|---|----|
| INTRODUCTION.....   | 5  |
| Topicality.....   | 5  |
| Aim and objectives.....   | 6  |
| Hypothesis.....   | 6  |
| Novelty.....  | 6  |
| Practical relevance.....  | 7  |
| Approbation of the research results.....  | 8  |
| Approbation of the research results at scientific conferences.....  | 8  |
| Other publications.....   | 9  |
| Structure of the Thesis.....  | 9  |
| 1. LITERATURE REVIEW.....   | 12 |
| 2. METHODOLOGY.....   | 15 |
| 2.1. Research design and methodological rationale.....  | 16 |
| 2.2. Materials and equipment.....   | 17 |
| 3. RESULTS.....   | 19 |
| 3.1. Comparison of two PCMs with melting temperatures 21 °C and 28 °C using hot plate<br>experiment (E1 – HP 21/28).....  | 19 |
| 3.2. Assessment of two PCMs with melting temperatures of 21 °C and 28 °C under steady-<br>state and dynamic laboratory conditions across different seasons (E2 – PCM 21/28).. | 20 |
| 3.3. Modelling in ANSYS Fluent – S1 and S2.....   | 22 |
| 3.4. Influence of adjustable insulation and heat-transfer elements – air gap, aerogel,<br>heat-transfer enhancer and Fresnel lens (E3 – ADJ ON/OFF).....                      | 23 |
| 3.5. Influence of dynamic component (E4 – DYN-LAB ON/OFF and E5 – DYN-LAB<br>ON/OFF).....   | 24 |
| 3.6. Effect of focal point distance and cone diameter on heat transfer within the small-scale<br>facade module (E6 – FP-LAB 3/5/7).....                                       | 26 |
| 3.7. Large-scale outdoor testing (E7 – TEST A/P/H).....   | 27 |
| 3.7.1. On-site testing.....   | 28 |
| 3.7.2. Power consumption of heat pumps.....   | 29 |
| 3.7.3. Determination of the effective thermal transmittance (U-value).....  | 30 |
| 3.7.4. Calculation of Energy-Comfort Performance Index.....   | 31 |
| 3.7.5. Conclusions and insights (E7 – TEST A/P/H).....  | 35 |
| CONCLUSIONS.....  | 39 |
| REFERENCES.....   | 42 |

# INTRODUCTION

## Topicality

The European Union's long-term vision to reach carbon neutrality by 2050, as defined in the European Green Deal [1], places unprecedented emphasis on accelerating the transition toward technologies that consume less energy and produce fewer CO<sub>2</sub> emissions. This challenge is particularly acute in the building sector, which is responsible for approximately 40 % of total energy consumption and 36 % of CO<sub>2</sub> emissions in the EU [2]. As a result, amendments to Directive 2010/31/EU on the energy performance of buildings and Directive 2012/27/EU on energy efficiency [3] call for a new generation of buildings – ones capable of delivering significantly better energy performance, integrating renewable energy systems and responding intelligently to environmental conditions. Increasing the role of on-site renewable energy is, therefore, highlighted as an essential decarbonisation pathway [4].

International climate policy documents, including the Intergovernmental Panel on Climate Change (IPCC) Assessment Reports, UNFCCC protocols and global climate agreements, repeatedly stress that reducing energy demand and improving energy efficiency are among the most effective mitigation measures for limiting global warming [5]. However, despite this recognition, the building sector continues to face major inefficiencies, with a substantial share of potential energy savings still unrealised [6]. Current projections indicate that global energy consumption may increase by 53 % over the coming decade, driven by demographic expansion, increasing comfort expectations, digitalisation and urbanisation, thereby further intensifying greenhouse gas emissions if no corrective measures are taken [7].

Conventional building designs – largely static in nature – are no longer adequate for meeting climate-neutrality targets. Most building envelopes are constructed using traditional insulation and fixed-performance facade elements, which do not respond dynamically to fluctuating outdoor conditions. Consequently, there is significant untapped potential for stored energy within facade elements to balance indoor thermal comfort during both heating and cooling periods, thereby improving the overall energy efficiency of the building. To address these limitations, a strong shift toward adaptive architectural solutions is emerging. Dynamic and kinetic facade systems, capable of responding to variations in solar radiation, temperature, wind, humidity and light [8], represent a promising direction for next-generation energy-efficient buildings.

In this broader policy and technological context, the EU Green Deal reinforces the need to pair renewable energy sources (RES) with intelligent control and energy management in buildings [1], [4], [9]. Nearly zero-energy buildings (nZEB) and the more recent concept of zero-emission buildings (ZEB), are now central pillars of European decarbonisation strategies. However, their practical implementation remains challenging because the availability of renewable energy rarely aligns with the building's actual energy demand. Unlike fossil-based systems, RES generation fluctuates daily and seasonally, creating periods of surplus production as well as intervals when supply is insufficient. These temporal mismatches make it difficult to ensure stable and efficient building operation, regardless of the season. Consequently,

innovative approaches to the building thermal envelope – especially solutions capable of storing and later releasing solar thermal energy – offer a promising pathway to improve the balance between renewable supply and building energy needs.

### **Aim and objectives**

The main goal of this Thesis is to develop an innovative adaptive facade system integrating thermal energy storage through the application of phase change materials (PCMs) and to evaluate its effectiveness in enhancing building energy performance. Achieving this aim requires a comprehensive investigation spanning conceptual development, experimental validation and numerical simulation. To fulfil this goal, the following research objectives have been established.

- 1) Conduct a systematic literature review covering thermal energy storage (TES) principles, PCM technologies, state-of-the-art insulation materials, adaptive facade concepts and existing experimental and numerical testing methodologies relevant to dynamic building envelopes.
- 2) In an iterative process, design and develop experimental prototypes, including a small-scale facade module for controlled laboratory investigations and a full-scale solar facade module integrated into outdoor test stands for real-environment performance evaluation.
- 3) Plan and execute experiments, ensuring controlled parameter variation, accurate instrumentation and reliable data acquisition under both steady-state laboratory and dynamic outdoor weather conditions.
- 4) Develop and validate numerical simulation models for the small-scale facade prototypes, enabling detailed heat-transfer analysis, performance prediction and comparative assessment with experimental data.
- 5) Collect, process and analyse measurement data to quantify the thermal performance, energy efficiency benefits and operational potential of the proposed adaptive facade solution, ultimately assessing its contribution to reducing heating and cooling energy demand.

### **Hypothesis**

The integration of phase change materials into an adaptive facade system will improve building energy efficiency by enabling controlled thermal energy storage and release, thereby reducing indoor temperature fluctuations and lowering heating and cooling demand across varying climatic conditions.

### **Novelty**

The novelty of this research lies in a paradigm shift of the building envelope not merely as a passive insulating barrier but as an active solar-thermal energy storage system. While dynamic and adaptive facade concepts have gained attention in recent years, their integration with PCMs

for seasonal and diurnal thermal storage remains underexplored, especially under real weather conditions characteristic of northern European climates.

This work advances the state of the art by:

- transforming the facade into a solar harvesting and storage unit, capable of absorbing, storing and releasing thermal energy through PCM phase transitions;
- addressing the critical challenge of renewable energy intermittency by embedding thermal buffering capacity directly into the building envelope;
- experimentally analysing the performance of PCM-integrated solar facades under dynamic boundary conditions, including outdoor testing under real climatic conditions, thereby providing data that are currently scarce in the literature;
- evaluating how such systems can reduce heating and cooling loads, thereby increasing on-site renewable energy utilisation and contributing to the transition toward zero-emission buildings by lowering operational greenhouse gas emissions;
- providing new insights into operational regimes, environmental impacts and adaptive potential of PCM-based dynamic envelopes, supporting the design of next-generation high-performance zero emission buildings.

Through this combined experimental and practical approach, the Thesis offers a novel pathway to bridge the gap between renewable energy availability on-site and building energy demand at the building thermal envelope level – something current static building systems cannot achieve.

## **Practical relevance**

The practical relevance of this research lies in its strong alignment with ongoing EU decarbonisation efforts, evolving building performance regulations and emerging architectural trends that emphasise adaptive and energy-responsive design. As EU member states progress toward transforming their building stock into nearly zero-energy or even positive-energy buildings, the demand for facade systems capable of dynamically responding to environmental conditions and significantly reducing energy use becomes increasingly critical. The PCM-integrated solar facade concept investigated in this Thesis directly addresses these needs by offering a multifunctional building envelope capable of harvesting, storing and redistributing solar thermal energy. Such systems have the potential to substantially reduce heating and cooling loads, enabling buildings to meet stringent EPBD requirements while lowering operational costs for occupants. By embedding thermal storage directly into the facade, buildings are able to use a greater share of on-site renewable energy during periods of availability, thereby decreasing reliance on fossil fuels and grid electricity during peak-demand hours. The approach is also highly scalable: it can be implemented in both new construction and deep renovation projects, which is essential for upgrading Europe's ageing building stock. Moreover, buildings equipped with facade-integrated thermal storage can function as energy-flexible assets within larger district energy systems, helping to mitigate the intermittency of renewable energy sources and contributing to overall grid stability. This research is particularly relevant in northern European climates, where heating demand is high and traditional solar

technologies often deliver limited benefits; the findings provide climate-specific insights into how dynamic solar-thermal facades can be effectively utilised even under low-sun conditions. In this way, the study advances both scientific understanding and practical deployment of adaptive envelope technologies, offering a viable pathway toward energy-positive, climate-neutral buildings and supporting the long-term objectives of the EU Green Deal.

### **Approbation of the research results**

1. Narbutis, J., Vanaga, R., Freimanis, R., Blumberga, A. Laboratory and outdoor testing of small-scale active solar facade module. *Environmental and Climate Technologies* 2021, vol. 25, no. 1, pp. 455–466. Available: doi: <https://doi.org/10.2478/rtuect-2021-0033>
2. Vanaga, R., Narbutis, J., Freimanis, R., Blumberga, A. Laboratory testing of small-scale solar facade module with phase change material and adjustable insulation layer. *Energies*. 2022, 15, 1158. Available: <https://doi.org/10.3390/en15031158>
3. Narbutis, J., Blumberga, A., Zundāns, Z., Freimanis, R., Bāliņš, R., Vanaga, R. The Effect of Fresnel Lens Focal Point Location on Heat Transfer in Phase Change Material (PCM) Enhanced Dynamic Solar Facade. *Environmental and Climate Technologies*, 2022, vol. 26, no. 1, pp. 1268–1278. e-ISSN 2255-8837. Available: doi:10.2478/rtuect-2022-0096
4. Vanaga, R., Narbutis, J., Zundāns, Z., Blumberga, A. On-site Testing of Dynamic Facade System with the Solar Energy Storage, *Energy*, 2023, vol. 283, 128257, ISSN 0360-5442. Available: <https://doi.org/10.1016/j.energy.2023.128257>
5. Vanaga, R., Narbutis, J., Freimanis, R., Zundāns, Z., Blumberga, A. Performance Assessment of Two Different Phase Change Materials for Thermal Energy Storage in Building Envelopes, *Energies*, 2023, vol. 16, no. 13, 5236. Available: <https://doi.org/10.3390/en16135236>
6. Narbutis, J., Vanaga, R. Revolutionizing the Building Envelope: A Comprehensive Scientific Review of Innovative Technologies for Reduced Emissions. *Environmental and Climate Technologies* 2023, vol. 27, no. 1, pp. 724–737. Available: <https://doi.org/10.2478/rtuect-2023-0053>
7. Vanaga, R., Narbutis, J., Zundāns, Z., Gušča, J. Systematic literature review of software tools for modeling heat transfer in phase change materials for building applications. *IOP Conference Series: Earth and Environmental Science*. 2024, 1372 012017. Available: <https://doi.org/10.1088/1755-1315/1372/1/012017>

### **Approbation of the research results at scientific conferences**

1. Vanaga, R., Narbutis, J., Freimanis, R., Blumberga, A. Laboratory testing of different melting temperature phase change materials under four-season conditions for thermal energy storage in building envelopes. *International Conference on Applied Energy* 2021, Nov. 29 – Dec. 2, 2021, Bangkok, Thailand.

2. Narbutis, J., Blumberga, A., Zundāns, Z., Freimanis, R., Bāliņš, R., Vanaga, R. The effect of Fresnel lens focal point location on heat transfer in phase change material (PCM) enhanced dynamic solar facade. *International Scientific Conference of Environmental and Climate Technologies Conect 2022*, May 11–13, 2022, Riga, Latvia.
3. Narbutis, J., Vanaga, R. Revolutionizing the Building Envelope: Innovative Technologies for Reduced Emissions. *International Scientific Conference of Environmental and Climate Technologies, CONECT 2023*, May 10–12, 2023, Riga, Latvia.
4. Narbutis, J., Vanaga, R., Zundāns, Z. Validating ANSYS Heat Transfer Models with Two Phase Change Materials. *International Scientific Conference of Environmental and Climate Technologies, CONECT 2024*, May 15–17, 2024, in Riga, Latvia.

### **Other publications**

1. Narbutis, J., Vanaga, R. Comparative Study of the Thermal Properties of Nanoparticle-Enhanced Phase Change Materials for Building Envelope Applications. *CONECT 2025. International Scientific Conference of Environmental and Climate Technologies*, 40. <https://doi.org/10.7250/CONECT.2025.017>
2. Narbutis, J., Vanaga, R. Nano-Enhanced Phase Change Materials for Building Envelopes: A Systematic Review of Thermal Performance and Applications. *Environmental and Climate Technologies 2023*, vol. 29, no. 1, pp. 359–389. Available from: <https://doi.org/10.2478/rtuect-2025-0025>

### **Structure of the Thesis**

The structure of this Doctoral Thesis is grounded in the paradigm shift from conventional to adaptive building envelopes, driven by the necessity to decarbonise the existing and future building stock. This transition is operationalised through three interlinked development cycles (see Fig. 1), which collectively form the methodological and conceptual backbone of the research.

Stage 1: Initial design optimisation of the technological solution and testing of PCM properties for computer simulations. This process leads to a technological concept and a preliminary small-scale prototype. Parallel to this, a numerical simulation model is developed to enhance understanding of heat transfer dynamics and identify energy-efficiency improvements.

Stage 2: Small-scale laboratory and outdoor testing, where the developed prototype undergoes performance evaluation under controlled and real environmental conditions.

Stage 3: Large-scale solar facade module development, where the prototype is transferred into a full-scale operational system for outdoor testing.

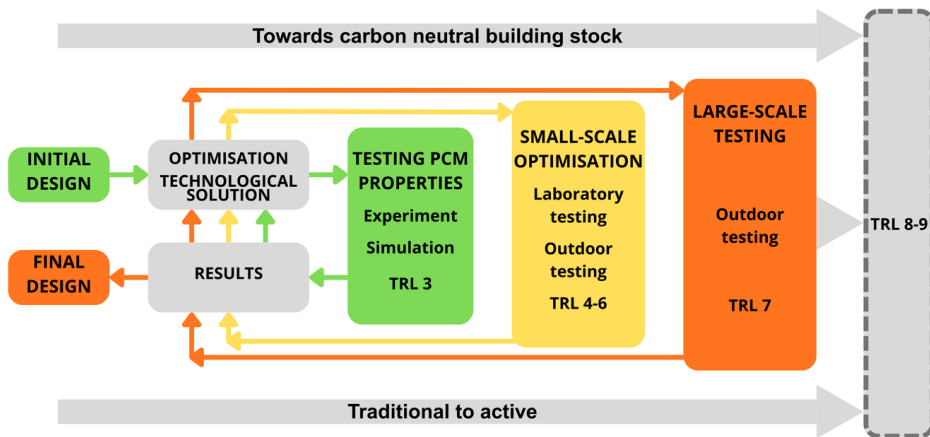


Fig. 1. Structure of the Thesis.

The Doctoral Thesis consists of seven chapters: (1) Introduction, (2) Literature Review, (3) Methodology, (4) Testing PCM Properties for ANSYS Simulations, (5) Small-scale Optimisation, (6) Large-scale Testing, and (7) Conclusions.

The Introduction presents the topicality of the research, aim and objectives, hypothesis, novelty, practical relevance, and the approbation of results.

The Literature Review provides a comprehensive synthesis of existing knowledge on thermal energy storage systems, PCMs, state-of-the-art insulation materials, adaptive facade systems and the methodologies used for experimental and numerical investigations.

The Methodology chapter outlines the structure and sequence of the experiments, numerical simulations, measurement instrumentation and materials employed in this Thesis.

Chapters 4–6 present the methodological approach combined with the results of each experiment and simulation. These chapters describe the findings obtained from laboratory tests, outdoor measurements and numerical simulations in a logical sequence aligned with the technological development cycles. Together, they demonstrate a clear and traceable progression of the proposed adaptive facade technology from conceptual development to full-scale implementation.

The Conclusions chapter summarises the main findings, discusses key insights and outlines future research directions.

Table 1 provides an overview of the scientific publications that form the scientific foundation of the Thesis and support the individual research components.

The AI tool (DeepL) was used to assist in translating and editing text to provide clarity and flow throughout the Thesis.

Table 1

## Scientific Articles used in Doctoral Thesis

| <b>Field</b>                                    | <b>Title of scientific research article</b>  |
|---|--|
| Literature review                               | Revolutionising the Building Envelope:<br>A Comprehensive Scientific Review of Innovative<br>Technologies for Reduced Emissions      |
|   | Systematic literature review of software tools for<br>modelling heat transfer in phase change materials<br>for building applications |
| Testing PCM properties<br>for ANSYS simulations | Performance Assessment of Two Different Phase Change<br>Materials for Thermal Energy Storage in Building Envelopes                   |
| Small-scale<br>optimisation                     | Laboratory Testing of Small-Scale Solar Facade Module with<br>Phase Change Material and Adjustable Insulation Layer                  |
|   | Laboratory Testing of Small-Scale Active Solar<br>Facade Module  |
|   | The Effect of Fresnel Lens Focal Point Location on<br>Heat Transfer in Phase Change Material (PCM)<br>Enhanced Dynamic Solar Facade  |
| Large-scale testing                             | On-site testing of a dynamic facade system with solar energy storage   |

# 1. LITERATURE REVIEW

The comprehensive literature review carried out in the Thesis establishes a coherent scientific, technological and policy-based foundation for the development of an adaptive solar facade system integrating phase change materials for thermal energy storage. The analysis has addressed six interrelated domains: EU building-stock policy, thermal energy storage principles, PCM technologies, high-performance insulation materials, adaptive building envelopes and experimental–numerical evaluation methodologies. Together, these domains define both the urgency of building-envelope innovation and the methodological pathway required to realise it.

The review of EU building-stock policy clearly demonstrates that the decarbonisation of the building sector is a central pillar of the European Green Deal and its associated legislative instruments, including the EPBD, the EED and the Renovation Wave Strategy. These frameworks collectively promote the transition toward ZEB, increased renovation rates, integration of on-site RES and the adoption of smart, adaptive building technologies. Since buildings account for a substantial proportion of final energy consumption and CO<sub>2</sub> emissions in Europe, improvements at the building-envelope level represent one of the most effective strategies for reducing operational energy demand. The policy context, therefore, directly supports the development of adaptive, energy-efficient and storage-integrated facade systems, confirming the scientific and societal relevance of this Thesis.

The investigation of TES technologies highlights the critical role of storage systems in enabling effective utilisation of intermittent renewable energy sources, particularly solar energy. LHTES, based on PCMs, offers significantly higher energy storage density than sensible heat systems and enables thermal energy to be stored and released at nearly constant temperatures. This characteristic makes PCMs particularly suitable for integration into building envelopes, where they can moderate indoor temperature fluctuations, shift peak loads and enhance solar-energy utilisation. The literature confirms that PCM-enhanced components can reduce heating and cooling demand, improve indoor comfort and support net-zero-energy building objectives. However, despite extensive laboratory research and small-scale applications, large-scale, long-term validation of PCM-integrated facade systems remains limited. This gap underlines the need for systematic experimental and numerical investigation at both component and building scales.

The analysis of PCM categories further clarifies the suitability of different materials for building integration. Solid–liquid PCMs, particularly paraffin-based organic materials, demonstrate favourable thermophysical properties, including appropriate melting-temperature ranges, stable cycling behaviour, low supercooling and chemical stability. Although inorganic and eutectic PCMs offer certain advantages, issues such as phase segregation and long-term stability require further optimisation. These findings support the material-selection strategy adopted in this Thesis, which focuses on PCMs appropriate for Northern European climatic conditions and seasonal performance variability.

High-performance insulation materials represent another essential component of advanced envelope design. The literature review identifies silica aerogels as one of the most promising

superinsulation technologies due to their ultralow thermal conductivity, lightweight nanoporous structure and potential for integration into multifunctional facade systems. Aerogels enable significant reductions in envelope thickness while maintaining high thermal resistance, making them particularly suitable for deep renovation and space-constrained applications. Although current cost levels and long-term hygrothermal durability require further research, life-cycle assessments indicate meaningful reductions in greenhouse gas emissions when aerogel-based systems are implemented. Their compatibility with PCM layers and adaptive facade concepts further reinforces the feasibility of hybrid envelope solutions combining insulation, thermal storage and solar management functions.

The review of adaptive building envelope technologies demonstrates a paradigm shift from static envelope components toward responsive, multifunctional systems capable of dynamically regulating thermal and solar performance. Smart glazing, kinetic shading devices, BiPV and PCM-enhanced facade systems illustrate the broad spectrum of adaptive solutions currently under development. Experimental and simulation-based studies show measurable reductions in cooling loads, improved photovoltaic efficiency and significant annual energy savings. Nevertheless, challenges remain regarding durability, cost-effectiveness, modelling reliability and system integration. These limitations highlight the importance of robust validation methodologies capable of capturing both steady-state and transient thermal behaviour under real climatic conditions.

In this context, the review of experimental testing methods confirms that traditional steady-state U-value measurements are insufficient for characterising adaptive and solar-responsive facade systems. Dynamic performance evaluation requires high-resolution monitoring of temperatures, heat fluxes and solar radiation under realistic outdoor conditions. The PASLINK methodology, evolved from the PASSYS project, provides a comprehensive experimental framework based on full-scale, highly instrumented test cells. By combining controlled indoor environments with exposure to natural climatic variations, PASLINK enables accurate determination of both steady-state and dynamic performance parameters. Its integration with system-identification techniques allows derivation of physically interpretable thermal resistances, capacities and solar-gain indicators. This methodology is particularly suitable for evaluating PCM-integrated adaptive solar envelopes and therefore forms a central component of the experimental strategy adopted in this Thesis.

Complementing experimental validation, computer simulation plays a fundamental role in the development and optimisation of innovative envelope systems. The seven-step simulation methodology identified in the literature provides a structured approach for linking conceptual design, performance indicators, modelling, benchmarking, optimisation and iterative refinement. High-fidelity numerical tools such as ANSYS Fluent, COMSOL, TRNSYS, MATLAB and EnergyPlus enable analysis of transient heat transfer, phase-change behaviour and whole-building energy performance. However, bibliometric analysis reveals that most PCM-related simulations are conducted at small scales and over short time periods, with relatively few studies addressing seasonal or annual performance at the building level. This gap is particularly relevant for adaptive solar envelopes intended to operate under highly variable Northern European climates. Consequently, the integration of multi-scale modelling by

combining detailed CFD analysis with long-term building energy simulations represents a key methodological advancement pursued in this research.

In conclusion, the literature review confirms that building-envelope innovation is central to achieving EU climate-neutrality objectives and that PCM-integrated adaptive solar facades represent a promising pathway toward enhanced energy efficiency and renewable-energy utilisation. At the same time, significant gaps persist in long-term validation, multi-scale modelling and full-system integration. By combining materials science, full-scale experimental testing and advanced numerical simulation within a structured methodological framework, this Thesis addresses these gaps and advances the development of adaptive, storage-enhanced solar envelope systems tailored to Northern European conditions.

## 2. METHODOLOGY

The methodological framework of this research is based on a systematic, multi-stage investigation of a dynamic solar facade system incorporating thermal energy storage using phase change materials. To evaluate the feasibility, performance and adaptability of the facade concept, the methodology integrates 3 stages (Fig. 2.1).

- 1) Testing PCM properties for ANSYS simulations: material-level experimental and numerical characterisation of PCM behaviour under controlled thermal loading.
- 2) Small-scale optimisation: component-level testing of small-scale facade modules using PASLINK-type laboratory and outdoor setups with simulated and real solar loads.
- 3) Large-scale outdoor testing: System-level outdoor comparative testing of a full-scale facade module in relevant climatic conditions.

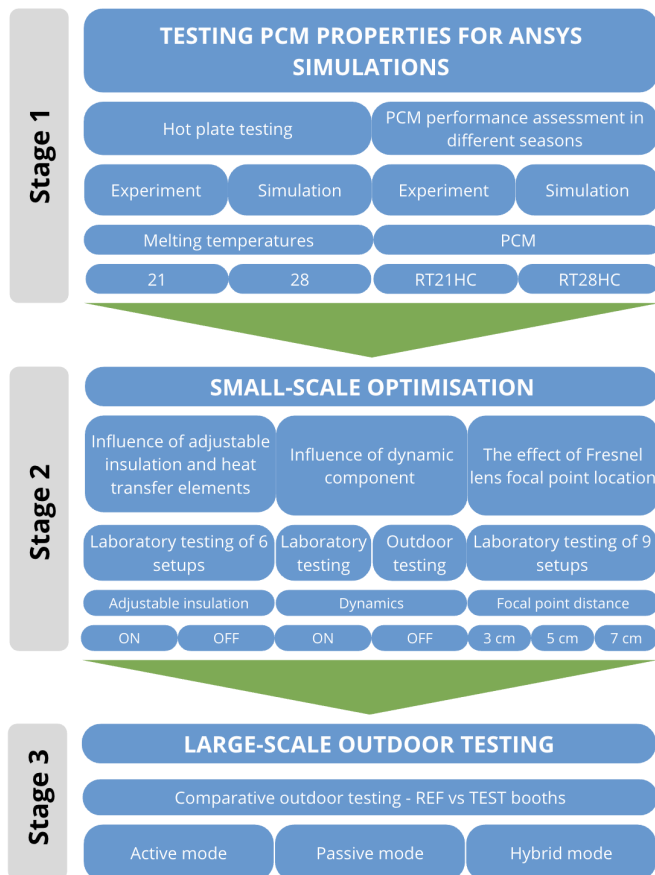


Fig. 2.1. Research methodology.

Together, these stages form an iterative design, testing and validation workflow that supports the development of the technology from conceptual design toward demonstration in

relevant environmental conditions. The following section presents the methodological choices, experimental setups, data acquisition systems, analytical tools and simulation approaches used throughout the research.

## 2.1. Research design and methodological rationale

A quantitative methodological approach was selected because the research required precise and reproducible evaluation of several key thermal parameters, including heat-flux dynamics, PCM charging and discharging behaviour, facade module performance under transient outdoor and simulated weather conditions, indoor temperature responses and associated impacts on heating and cooling energy consumption. All experimental investigations generated high-resolution, time-dependent datasets containing temperatures, heat fluxes, solar irradiance measurements and energy-consumption data. These datasets enabled robust statistical analysis, accurate parameter identification, and reliable calibration and validation of the numerical models developed later in the study.

PASLINK-type testing plays an essential role within this methodology because the behaviour of PCM-based dynamic facades cannot be adequately assessed using steady-state analysis. PCMs exhibit hysteresis, rate-dependent phase transitions and varying storage efficiencies depending on the interaction between indoor-outdoor temperature gradients and solar input. PASLINK setups enable controlled indoor boundary conditions while allowing fully dynamic external exposure, thus creating a measurement environment that captures the transient nature of PCM behaviour. The PASLINK approach also supports long-duration monitoring, which is crucial for analysing multi-day charging and discharging cycles, diurnal patterns and seasonal effects that influence the operational viability of PCM-integrated facade systems.

The experimental study (Table 2.1) comprised seven physical experiments and two numerical simulation studies. These included PCM hot-plate tests, seasonal simulations of PCM behaviour using small-scale PASLINK setups, laboratory and outdoor assessments of dynamic optical components, optimisation of Fresnel lens focal point positioning and large-scale facade evaluation using PASLINK outdoor test booths. Numerical simulations complemented these tests by modelling PCM phase-transition processes, solar-concentration effects and heat transfer under various climatic conditions.

Table 2.1

Overview of the Experimental Study

| Stage | Denotation        | Experiment / simulation                   | Type                              | Data obtained                  | Aim  |
|-------|-------------------|---|-----------------------------------|--------------------------------|--|
| 1     | E1 – HP<br>21/28  | Hot-plate experiment                      | Small-scale laboratory experiment | Temperatures, heat fluxes      | Comparison of melting temp.: 21 °C vs 28 °C  |
|       | E2 – PCM<br>21/28 | Experiment: PCM performance assessment in | Small-scale comparative PASLINK   | Temperatures, solar irradiance | PCM performance evaluation: RT21HC vs RT28HC |

| Table 2.1 (continued) |                               |  |   |   |   |
|-----------------------|-------------------------------|--|---|---|---|
|                       |                               | different seasons  | laboratory experiment                                 |   |   |
|                       | <b>S1</b> – HP<br>21/28       | Hot-plate simulation   | Small-scale simulation                                | Temperatures, melting/solidification                            | Calibration of the PCM model for S2                   |
|                       | <b>S2</b> – PCM<br>21/28      | Simulation: PCM performance in different climate zones                           | Small-scale simulation                                | Temperatures, melting/solidification                            | PCM performance evaluation: RT21HC vs RT28HC          |
| <b>2</b>              | <b>E3</b> – ADJ<br>ON/OFF     | Experiment: Influence of adjustable insulation layer                             | Small-scale comparative PASLINK laboratory experiment | Temperatures, heat fluxes                                       | Evaluation of adjustable insulation: ON/OFF           |
|                       | <b>E4</b> – DYN-LAB<br>ON/OFF | Experiment: Influence of the dynamic component                                   | Small-scale comparative laboratory experiment         | Temperatures, heat fluxes                                       | Evaluation of the dynamic component: ON/OFF           |
|                       | <b>E5</b> – DYN-OUT<br>ON/OFF | Experiment: Influence of the dynamic component (outdoor)                         | Small-scale comparative outdoor experiment            | Temperatures, heat fluxes, solar irradiance                     | Evaluation of the dynamic component: ON/OFF           |
|                       | <b>E6</b> – FP-LAB<br>3/5/7   | Experiment: Fresnel lens focal point optimisation                                | Small-scale comparative laboratory experiment         | Temperatures, solar irradiance                                  | Identification of focal-point distance: 3/5/7 cm      |
| <b>3</b>              | <b>E7</b> – TEST<br>A/P/H     | Experiment: On-site testing of a dynamic facade system with solar-energy storage | Large-scale comparative outdoor experiment            | Temperatures, heat fluxes, solar irradiance, energy consumption | Evaluation of performance: Active/passive/hybrid mode |

## 2.2. Materials and equipment

This research employed a combination of controlled laboratory infrastructure, custom-built test stands and multiple generations of facade module prototypes to experimentally evaluate the thermal performance of PCM-enhanced dynamic solar facades. The materials and equipment described in this section represent the physical components of the facade modules themselves, as well as the environmental systems used to impose well-defined and repeatable boundary conditions. The aim is therefore to describe the structural materials, phase-change media, solar-concentration elements, insulation components and experimental test stands that formed the basis of all investigations.

Two commercially available paraffin-based PCMs (RT21HC and RT28HC) were used throughout the research. These were selected because their melting temperatures align with indoor thermal-comfort ranges and are highly suitable for facade-integrated latent heat storage applications. RT21HC has a melting temperature of approximately 21 °C and is characterised by a high latent heat capacity and a narrow phase-transition range, enabling effective thermal buffering during diurnal charging-discharging cycles. RT28HC, with a melting temperature of

around 28 °C, was used to assess the impact of higher transition temperatures under both cold-season and warm-season outdoor conditions.

Both PCMs were encapsulated in rectangular glass containers whose external dimensions varied between experiments; however, the internal geometry remained constant within each experiment to ensure comparability. In several module generations, copper plates or rods were incorporated into the PCM containers to enhance internal heat transfer and reduce thermal stratification during the phase-transition process.

Multiple insulation strategies were tested. Silica aerogel insulation was used extensively as a high-performance, translucent, low-density insulating layer. Aerogel was applied fully, partially, or within dynamic components such as reflective blades or cone-shaped optical elements. Air gaps (flat and conical) were used to manipulate convective heat transfer and influence the solar-concentration pathway. Cone-shaped air gaps with PMMA or Fresnel lenses on the exterior were key features in experiments investigating the influence of cone geometry and focal-point position on PCM charging efficiency. Additionally, an adjustable insulation layer was applied during nighttime discharging in certain laboratory experiments to reduce heat losses without hindering daytime charging.

Optical components played a central role in the dynamic facade modules. PMMA covers acted as transparent protective layers in non-concentrating configurations, allowing unaltered solar radiation to reach the PCM while providing mechanical stability. Fresnel lenses, also made from PMMA, were used in concentrating configurations to intensify solar radiation on the PCM container and significantly increase charging temperatures. Their positioning relative to the PCM surface was varied to identify optimal focal-point alignment.

All laboratory experiments were conducted using manually constructed testing stands within controlled environmental chambers capable of reproducing both steady-state and dynamic seasonal conditions. Outdoor experiments were carried out on the rooftop of Riga Technical University (Riga, Latvia), on custom-built stands directly facing South. The methodological approach, test-stand design, specific experimental procedures and results for each investigation are described in detail in the following chapters.

### 3. RESULTS

#### 3.1. Comparison of two PCMs with melting temperatures 21 °C and 28 °C using hot plate experiment (E1 – HP 21/28)

An experimental stand for the hot plate testing is presented in Fig. 3.1.

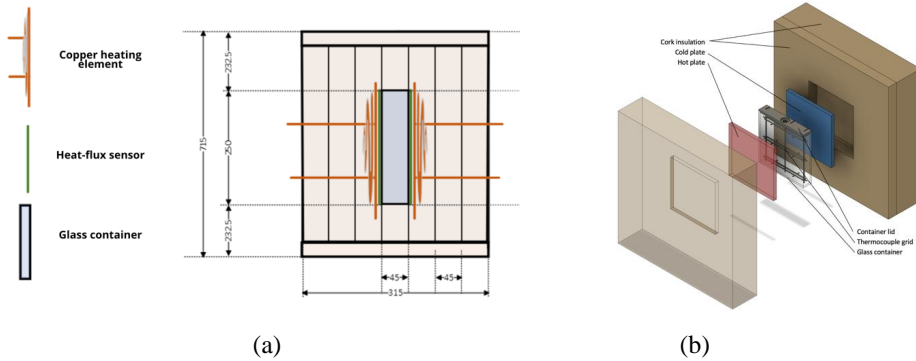


Fig. 3.1. Experimental stand for the hot plate test: (a) cross-section of the apparatus and (b) schematic of the component layout.

A 12-round experiment was carried out according to the settings specified in Table 3.3. The first four rounds were conducted under steady-state conditions to determine the thermal conductivity ( $\lambda$ ) of the PCM. From rounds 5 to 12, dynamic experiments were carried out using the hot plate apparatus. The calculated results for these steady-state measurements are summarised in Table 3.1. The resulting representative conductivity values are 0.255 W/(m·K) for RT21HC and 0.3 W/(m·K) for RT28HC.

Table 3.1

Experimentally Measured Values and Calculated Thermal Conductivity

| Round | PCM    | Stabilisation time, h | $q$ – measured heat flux, W/m <sup>2</sup> | Hot plate temp., T <sub>HP</sub> [°C] | Cold plate temp., T <sub>CP</sub> [°C] | L – sample thickness, m | $\lambda$ – thermal cond., W/(m·K) |
|-------|--------|-----------------------|--|---------------------------------------|--|-------------------------|------------------------------------|
| 1     | RT21HC | 15                    | 82.12                                      | 28.27                                 | 9.68                                   | 0.056                   | 0.25                               |
| 2     |        | 22                    | 91.46                                      | 29.57                                 | 9.67                                   | 0.056                   | 0.26                               |
| 3     | RT28HC | 10                    | 94.5                                       | 34.74                                 | 17.69                                  | 0.056                   | 0.31                               |
| 4     |        | 53                    | 89.80                                      | 34.90                                 | 17.71                                  | 0.056                   | 0.29                               |

The experimental investigation of two PCMs using a hot plate apparatus across twelve rounds provided comprehensive insights into their thermal characteristics and behaviour under controlled heating and cooling cycles. The main conclusions from this stage of the research are as follows.

- 1) Initial verification tests with reference materials – XPS and fibrolith – confirmed the accuracy and reliability of the hot plate apparatus. The experimentally obtained thermal

conductivity values were consistent with datasheet values, thereby validating the calibration procedure and compliance with standardised measurement protocols.

- 2) The HFM method enabled experimental determination of the effective thermal conductivity of RT21HC and RT28HC throughout their phase transition cycles (melting and solidification). These experimentally derived  $\lambda$ -values serve as essential input parameters for subsequent numerical modelling of PCM behaviour.
- 3) RT21HC exhibited a relatively stable thermal response during both heating and cooling stages. Nevertheless, moderate asymmetry in plate temperatures and corresponding heat fluxes was observed in several rounds, primarily due to insufficient cooling performance on Plate 2. Thermal and heat-flux stabilisation typically occurred after 15–31 hours, reflecting the expected lag associated with latent heat absorption and release.
- 4) RT28HC demonstrated comparable heat absorption dynamics but showed slightly greater sensitivity to boundary-condition variations. Round 10 produced the most stable thermal environment of the entire testing, with nearly identical plate temperatures and heat-flux profiles – underscoring the value of well-balanced thermal boundaries for accurate PCM characterisation.
- 5) A recurring limitation across multiple rounds was the inadequate cooling of Plate 2, which hindered the system from reaching the desired setpoint temperatures (e.g., 2 °C) during cooling cycles. This imbalance resulted in non-uniform thermal fields and incomplete PCM solidification, affecting the precision of phase-transition evaluation.
- 6) The findings highlight the critical importance of precise temperature control and symmetric boundary conditions in PCM testing. Even small discrepancies in plate temperatures produced measurable deviations in heat flux and extended stabilisation periods, potentially influencing the accuracy of extracted thermal properties.
- 7) Despite the noted operational constraints, the hot plate apparatus proved to be an effective tool for assessing PCM thermal behaviour for building-envelope applications. It enabled detailed observation of melting/solidification processes, heat-flux evolution and stabilisation times under controlled thermal gradients.
- 8) The extensive dataset generated over the twelve experimental rounds provides a robust foundation for developing and validating numerical models capable of simulating PCM-enhanced systems under dynamic thermal loads.

### **3.2. Assessment of two PCMs with melting temperatures of 21 °C and 28 °C under steady-state and dynamic laboratory conditions across different seasons (E2 – PCM 21/28)**

In Fig. 3.2, small-scale PASSLINK-type test cell dimensions and experimental setup are presented. Figure 3.3 presents a comparison of the maximum average temperatures reached by both PCMs and the corresponding indoor air temperatures under steady-state and dynamic testing conditions. Although the overall temperature trends are similar across the two experimental modes, the absolute values recorded in the steady-state tests are higher, primarily due to the absence of irradiance interruptions during these runs.

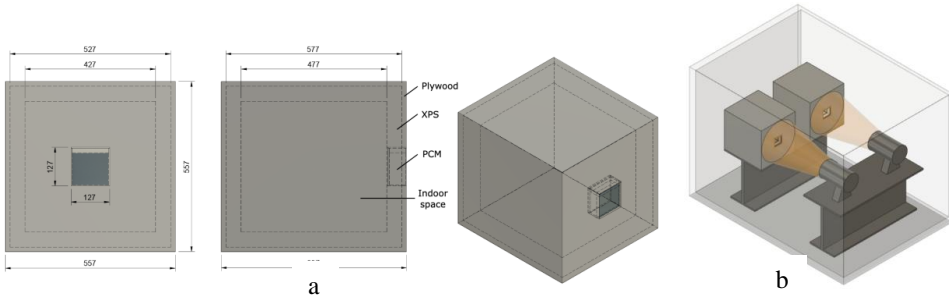


Fig. 3.2. Small-scale PASSLINK-type test cell (a) and experimental setup (b).

Across autumn, winter and spring conditions, RT28HC consistently achieves higher peak PCM temperatures. However, despite these higher PCM temperature peaks, RT21HC systematically results in higher indoor air temperatures in all seasons and in both experimental modes. This indicates that RT21HC is more effective in storing thermal energy within the PCM layer and subsequently releasing it into the interior environment, thus providing superior thermal performance.

Further analysis reveals that RT21HC maintains higher indoor temperatures with a noticeably gentler decline during the discharging phase, demonstrating a more stable release of stored heat. In contrast, RT28HC exhibits higher temperature peaks during the charging phase but undergoes a sharper temperature drop once the solar simulator is switched off. This behaviour reflects a predominance of sensible rather than latent heat storage in RT28HC under the tested conditions.

Layer-specific temperature measurements confirm these observations: in the majority of cases, all layers of RT21HC enter the melting range and participate in latent heat storage, whereas none of the RT28HC layers reaches the melting point during comparable conditions, showing only oscillations between minimum and maximum temperatures during the charging cycle.

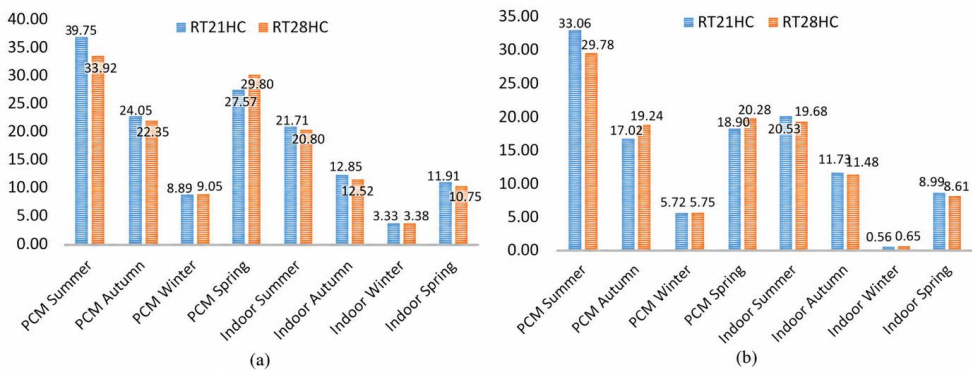


Fig. 3.3. Comparison between the highest temperatures reached by RT21HC and RT28HC in (a) steady-state test and (b) dynamic test.

In the summer setup, both PCMs reach the melting point, yet the temperature evolution remains characteristic: RT21HC shows a more gradual temperature rise and retains higher temperatures during the night, while RT28HC exhibits sharper fluctuations due to partial melting and sensible heat dominance.

Overall, the experimental results demonstrate that, under the tested climate conditions, RT21HC provides more efficient thermal energy storage and a more favourable thermal contribution to indoor temperatures compared to RT28HC, particularly in transitional seasons where partial melting plays a key role in performance.

### 3.3. Modelling in ANSYS Fluent – S1 and S2

Figure 3.4 represents schematics of S1 and S2 simulation models in ANSYS Fluent.

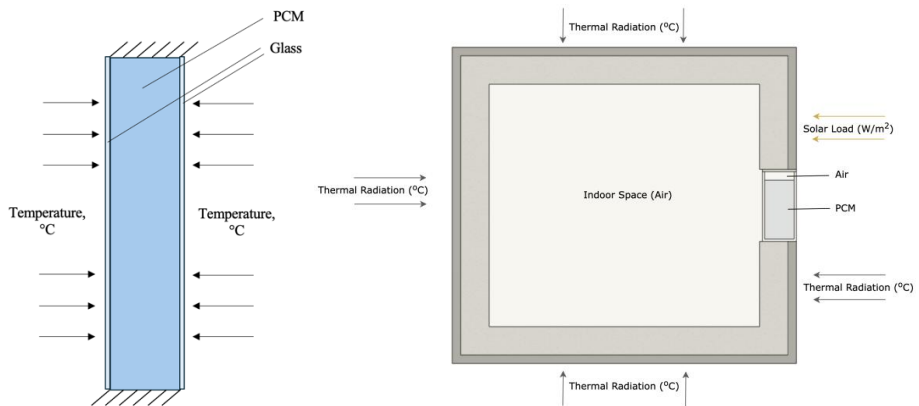


Fig. 3.4. Schematic of S1 (left) and S2 (right) simulation models.

The ANSYS Fluent model developed in simulation S1 successfully reproduced the overall thermal behaviour of both PCMs (RT21HC and RT28HC) under controlled hot-plate conditions and was validated against eight experimental rounds. The comparison revealed that the numerical model performs with high accuracy when boundary conditions are stable and moderate, particularly during low-intensity heating and cooling in both materials. Under these conditions, the RMSE and RRMSE values remain low, and the correlation between simulated and measured temperatures is strong (e.g.,  $R^2 = 0.87$  for RT21HC heating). In contrast, significant discrepancies arise during extreme thermal transitions (cooling to 2 °C or heating above 45 °C), where experimental plate temperatures could not consistently reach or maintain the prescribed setpoints. These boundary inconsistencies delay or suppress phase transitions in the physical PCM and lead to systematic deviations in the simulation, which responds ideally and therefore predicts faster melting or solidification. Despite these limitations, the long-term thermal trends and equilibrium temperatures between simulation and experiment show good agreement, demonstrating that the calibrated material properties and numerical approach provide a physically reliable representation of PCM behaviour.

Simulation S1 establishes a validated modelling framework that captures the dominant heat transfer mechanisms and phase-change dynamics, while also identifying the sensitivity of PCM behaviour to imperfect boundary control. These insights directly inform the transition to simulation S2, in which the small-scale PCM test-box model is developed to evaluate RT21HC and RT28HC under real climatic boundary conditions. Because S2 involves spatially distributed solar gains, diurnal temperature cycles and climate-dependent charging/discharging behaviour, the validated S1 material parameters and heat-transfer settings provide a robust foundation. The observed differences between simulated and experimental phase-change rates in S1 motivate the inclusion of climate-specific transient boundary conditions in S2, enabling a more accurate comparison of the two PCMs across representative weather profiles and seasons.

The S2 small-scale PCM test box simulation demonstrates that PCM performance is strongly dependent on climate zone, seasonal temperature profiles and solar irradiance intensity. Across all simulated climates, RT28HC consistently provides more stable thermal behaviour than RT21HC due to its higher melting temperature and greater latent heat capacity. In mild and moderate climates (Helsinki spring/autumn), both PCMs partially melt, but RT21HC retains heat more effectively during the discharge phase. In high-irradiance climates (Seville spring), RT21HC overheats, whereas RT28HC maintains indoor temperatures within the comfort range. Under winter conditions in Seville, both PCMs demonstrate similar storage capacity, though RT28HC performs slightly better. In Helsinki summer, both PCMs melt, but RT28HC suppresses overheating more efficiently.

These findings confirm that RT21HC is better suited for colder northern climates where the risk of overheating is minimal, whereas RT28HC provides superior performance in warmer or high-irradiance regions. Nonetheless, the limited internal volume of the small-scale test box remains a major constraint for fully evaluating the behaviour of a building envelope under real operating conditions.

### 3.4. Influence of adjustable insulation and heat-transfer elements – air gap, aerogel, heat-transfer enhancer and Fresnel lens (E3 – ADJ ON/OFF)

Figure 3.5 represents the experimental test box and setup for E3.

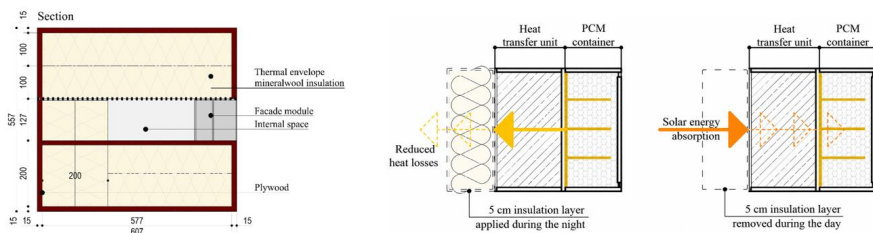


Fig. 3.5. Small-scale PASLINK type test box (left) and experimental setup of façade module (right).

Results show that applying the adjustable insulation layer increased average temperatures in both the PCM and the “indoor space” across all setups. However, the most significant impact was observed in modules featuring an air-gap layer, where the additional insulation most effectively reduced heat loss during the discharging phase. These modules demonstrated superior performance compared to more heavily insulated configurations, as their temperature curves converged more closely after solidification, indicating slower heat dissipation and improved thermal retention.

Overall, when considering the complete thermal cycle (charging and discharging), modules containing an air-gap layer gained and released more energy than the other configurations. In contrast, modules equipped with higher levels of fixed insulation demonstrated advantages primarily in latent heat storage, showing more stable temperature plateaus during phase transition.

It is important to note that the relatively small size of the test stand contributed to elevated PCM and indoor temperatures in all configurations. For this reason, the following stage of the research focuses on scaling the system to a larger format and validating its behaviour under realistic environmental conditions.

The comparative evaluation – based on multiple reference points such as indoor temperature and average PCM temperature at 24 and 48 hours, with and without the adjustable insulation – confirmed that the choice of configuration should depend on the intended functional objective of the solar facade. For instance, setups with an air-gap layer demonstrated the fastest melting rate and highest temperatures under the tested conditions, making them suitable for locations with short periods of solar exposure. Conversely, more insulated setups may be better suited for orientations with high solar loads, where controlling excessive sensible heat gains becomes important.

These insights directly inform the next steps of the research. In experiments E4 and E5, attention shifts to evaluating the influence of the dynamic component, both in laboratory conditions and in outdoor testing. The findings from the present experiment highlight the thermal sensitivities and energy-storage dynamics of different PCM-insulation configurations, which are essential for interpreting the behaviour of the dynamic facade module. As the system transitions from passive PCM-insulation optimisation (this experiment) to active solar-tracking and outdoor operation (E4–E5), the identified thermal patterns, phase-change characteristics and system sensitivities provide a foundational reference for assessing how dynamic sunlight concentration, blade motion and real-weather loads further enhance or alter the PCM performance.

### **3.5. Influence of dynamic component (E4 – DYN-LAB ON/OFF and E5 – DYN-LAB ON/OFF)**

The main advancement compared with the previous study is the integration of a dynamic component consisting of rotating blades. This component serves two primary functions:

- light concentration, directing incident solar radiation toward the heat-transfer element to increase energy input to the PCM;

- thermal insulation, as the blade interiors are filled with aerogel to reduce heat losses from the module during the discharging phase (adjusted insulation).

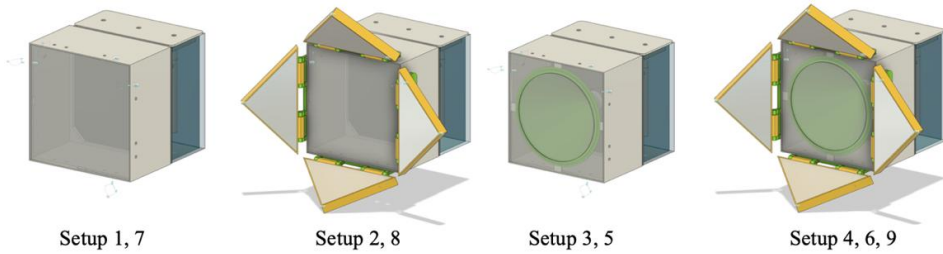


Fig. 3.6. Drawings of solar facade module in different setups.

To identify the optimal combination of materials and geometric parameters, the module was tested in several configurations (see Fig. 3.6).

Figure 3.7 presents a comparison of the average PCM temperatures for all nine experimental configurations.

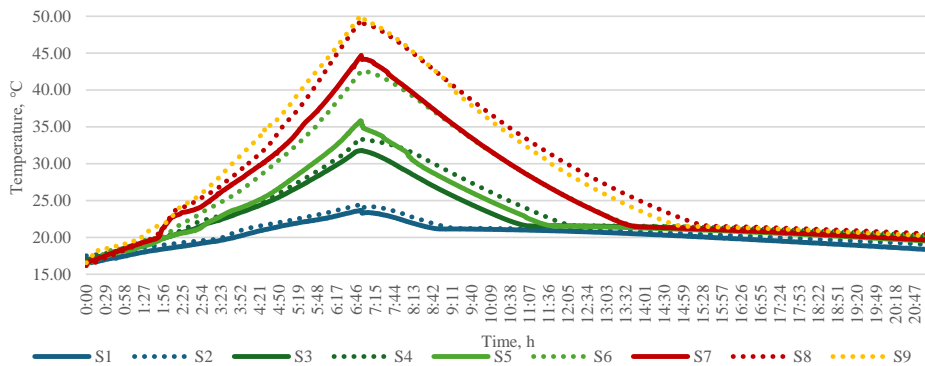


Fig. 3.7. Comparison of the average PCM temperatures for experimental configurations.

The combined results of the laboratory investigation (E4) and the outdoor testing (E5) demonstrate a consistent and measurable advantage of the dynamic component – comprising reflective blades with an aerogel-filled structure – within the proposed solar facade module. Under controlled laboratory conditions, the dynamic component significantly enhanced thermal energy absorption during the PCM charging phase and improved heat retention in the discharging phase. This improvement was especially evident in setups where the cone, aerogel layer and adjustable insulation were optimised to facilitate heat transfer from the Fresnel lens to the PCM.

Introducing the Fresnel lens further increased the concentration and intensity of solar gains, producing a more dynamic thermal response in the PCM. The combined action of the reflective blades and the Fresnel lens reduced thermal losses, accelerated PCM melting in upper and lower layers and extended the duration of effective thermal discharge. The laboratory results confirm

that both geometrical configuration and component interaction play a crucial role in determining the overall thermal efficiency of the solar facade module.

Outdoor experiments reinforced these findings under real climatic conditions. Even with fluctuating solar irradiance, variable solar angles and intermittent cloud cover, the facade module equipped with the dynamic component (Setup 10) outperformed the static version (Setup 11). The dynamic configuration achieved higher PCM temperatures, smoother heat-flux profiles and more effective heat storage during late-day conditions when the sun's azimuth angle shifted westward – highlighting the operational benefit of blade actuation. The improved performance during the discharging period further confirmed that strategic concentration and insulation elements reduce the rate of heat loss and extend the usable storage period.

Together, the results of E4 and E5 demonstrate that the performance of the facade module is highly sensitive to how effectively the optical and thermal components – reflective blades, cone, aerogel insulation and Fresnel lens – work together to direct and retain solar energy. While the positive influence of the Fresnel lens was clearly observed, the experiments also indicated that its effectiveness depends strongly on the precise location of the focal point relative to the aerogel layer, cone geometry and PCM container. These insights provided the foundation for the next stage of development – Experiment E6 – in which the focal point position of the Fresnel lens is systematically evaluated.

### 3.6. Effect of focal point distance and cone diameter on heat transfer within the small-scale facade module (E6 – FP-LAB 3/5/7)

The final component-level laboratory experiment, conducted to complete the development of the small-scale module intended for integration into a full-scale facade system, focused on determining the optimal focal-point position and cone diameter. The custom-designed small-scale solar facade module constructed for this purpose comprises several key elements (see Fig. 3.8): a dynamic component with movable reflective blades filled with aerogel insulation; a Fresnel lens; a concentrating cone; a semi-transparent aerogel insulation layer; a PCM container; and a transparent glass shell enclosing the aerogel layer.

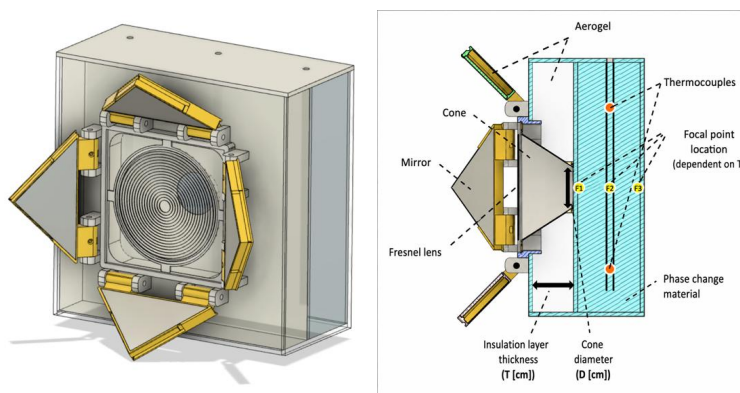


Fig. 3.8. Design of the small-scale solar facade module and its cross-section.

The obtained PCM temperature results allow the following conclusions:

1. The highest daytime heat transfer is achieved in Setup F1 D4, where the maximum PCM temperature reaches 19.52 °C during the daytime cycle.
2. The highest end-of-cycle PCM temperature is observed in the setup with the narrowest cone diameter, differing by 7.5 % from the lowest-performing setup. This indicates the lowest night-time heat losses in Setup F3 D2.
3. By shifting the focal point deeper into the PCM container, effective heat transfer is achieved with narrower cone diameters. Comparing Setups F1 D4 and F3 D2, the difference in average PCM temperature is only about 3 %.
4. Heat-transfer enhancement during the charging phase can be accomplished with a wide cone and a thin aerogel layer (F3); however, increased heat losses during the nighttime cycle may reduce the overall benefit. For example, in Setup F3 D3, the second-highest daytime temperature (19.16 °C) drops to the second-lowest end-of-cycle value (16.45 °C).
5. Both focal point location and cone diameter significantly affect heat-transfer performance. Comparing Setups F1 D2 and F1 D4, the average PCM temperature increases by 7.2 %. Similarly, comparing F3 D4 and F1 D4 yields a 5.4 % increase.

The experiments indicate that Setup F1 D4 provides the best overall performance. However, when integrating the module into the dynamic solar envelope, the final focal point distance must also consider the aerogel insulation thickness, since this layer directly affects nighttime heat losses. The obtained results show that wider cone diameters enhance heat transfer; therefore, for the developed solar facade, the most suitable configuration combines a 7 cm aerogel insulation layer with focal point location F1.

### **3.7. Large-scale outdoor testing (E7 – TEST A/P/H)**

In this section, the evolution of the final methodological stage, experimental testing, has been presented and discussed. This stage of testing involves a system-level outdoor comparative experiment of a full-scale facade module in relevant climatic conditions. The main goal of this experiment is the evaluation of indoor thermal fluctuations and energy consumption across seasons to gain insights and conclusions about the energy efficiency of the proposed technological solution – dynamic solar envelope.

Large-scale outdoor experimental testing stands are represented in Fig. 3.9.

The concept for the large-scale solar facade module builds upon the configuration developed in the small-scale experiments by assembling nine small-scale units into a unified building-envelope component. For performance comparison, a triple-glazed window was selected as the reference technology. This choice aligns with the primary functional objectives of the proposed system, such as light transmission and heat conservation.



Fig. 3.9. Testing (left) and reference (right) stands (a); solar facade system containing nine small-scale dynamic modules from outside (b) and inside (c) testing booth.

### 3.7.1. On-site testing

To comprehensively evaluate the experimental data and derive meaningful conclusions regarding the performance of the test stand, a set of comparison criteria was established to assess differences between the test and reference booths:

- temporal comparison – experimental results were analysed over 24-hour periods to capture full day–night cycles;
- thermal performance – evaluation was based on how effectively indoor temperatures were maintained within the comfort range of 15–25 °C.
- energy efficiency – assessment was performed according to the electrical consumption of the heat pumps across all operating regimes.

Using these criteria, representative 24-hour periods were selected to ensure a robust and meaningful performance analysis. The chosen days cover all operational modes of the dynamic solar facade and span a wide range of climatic conditions, including both sunny and overcast days in all four seasons.

Day selection was based on data from the local meteorological station, particularly measured solar irradiance and outdoor temperature. A complete list of the selected days used for detailed evaluation is provided in Table 3.2.

Table 3.2

List of Selected Days for Experimental Data Evaluation Based on Weather, Season and Regime

|                                | Winter | Sunny weather | Cloudy weather |
|--------------------------------|--------|---------------|----------------|
| Passive                        |        | X             | X              |
| Active                         |        | X             | 15/02/2023     |
| Passive (day)–Active (night)   |        | 14/02/2023    | 22/02/2025     |
|                                | Spring | Sunny weather | Cloudy weather |
| Passive                        |        | 19/04/2025    | 14/03/2023     |
| Active                         |        | 14/05/2023    | 16/05/2023     |
| Passive (day) – Active (night) |        | 5/05/2025     | 6/05/2025      |
|                                | Summer | Sunny weather | Cloudy weather |
| Passive                        |        | 8/07/2024     | 5/07/2024      |
| Active                         |        | 22/08/2024    | 23/08/2024     |
| Passive (day) – Active (night) |        | 26/06/2025    | 24/06/2025     |
|                                | Autumn | Sunny weather | Cloudy weather |
| Passive                        |        | 22/09/2023    | 23/09/2023     |
| Passive (day) – Active (night) |        | 16/10/2024    | 14/10/2024     |
| Passive (night) – Active (day) |        | 7/09/2024.    | X              |

### 3.7.2. Power consumption of heat pumps

Power consumption data for the years 2023 and 2024 are graphically presented in Figs. 3.10 and 3.11, respectively.

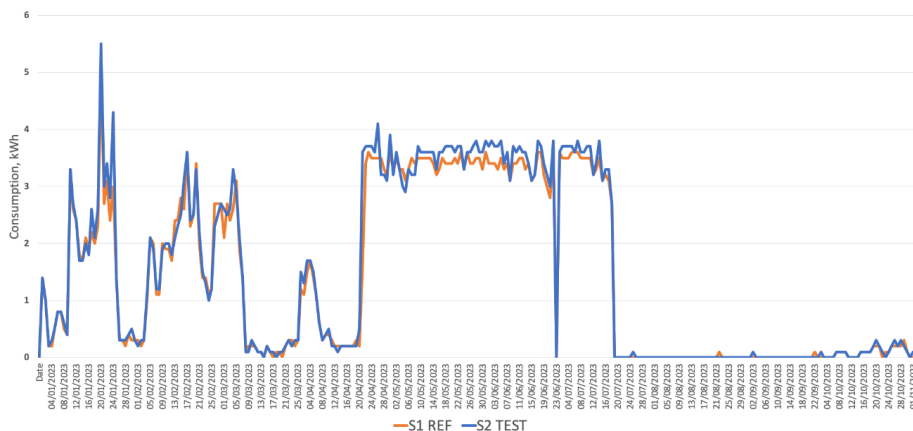


Fig. 3.10. Power consumption of heat pumps from 4 January to 1 November in 2023.

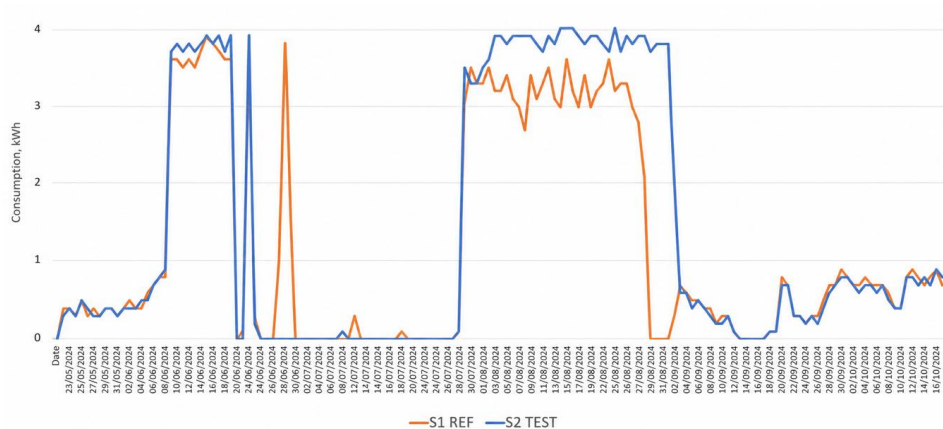


Fig. 3.11. Power consumption of heat pumps from 23 May to 16 October in 2024.

In the graphs, the labels “S1 REF” and “S2 TEST” correspond to the heat pumps in the reference and test stands, respectively. As expected, seasonal variation strongly influences the energy consumption of both heat pumps. In 2023, the consumption curves for both stands generally follow a similar pattern; however, the test stand (S2) consistently consumes slightly more energy to maintain the desired indoor temperature. A notable peak consumption is observed during the winter period, particularly on 23 January, when the test stand’s energy use exceeds 5 kWh. During the spring and summer months (April to July 2023), both systems display a relatively steady consumption trend, typically ranging between 3 and 4 kWh per day. Intervals with near-zero consumption indicate periods when the heat pumps were deactivated. In 2024, the heat pump energy consumption follows a similar seasonal pattern. However, during the period from 1–29 August, the test stand operates continuously and consumes approximately 1 kWh more energy per day than the reference stand. From 3 September to 16 October, the system was tested in various operational regimes, with the heat pumps running either only during the day or only at night. During this period, the trend reverses slightly, with the test stand consuming marginally less energy than the reference stand, suggesting improved efficiency under alternating operation modes.

### 3.7.3. Determination of the effective thermal transmittance (U-value)

The correctness of the computed U-value depends critically on the assumption that the facade system is behaving as a purely conductive element during the analysed period. For PCM facades, this requires confirming that the PCM remains in the solid or liquid state and that no melting or solidification occurs that would complicate the heat flux signal with latent heat effects. This was verified independently using PCM container temperature measurements, which showed that in the winter, spring and autumn dates analysed, all PCM temperatures remained well below the melting range and summer dates were well above it (19–21 °C for RT21HC). In addition, no heating, cooling or ventilation systems were operating in the booths during these experiments, ensuring that the thermal environment was governed solely by the

natural indoor-outdoor temperature difference and internal radiative equilibrium. The solar facade module was also inactive during these calculated periods (dynamic elements were in closed position), and solar irradiance was not present to introduce appreciable solar charging into the PCM. Calculated nighttime U-values are listed in Table 3.3.

Table 3.3

Calculated Steady-State U-Value at Night

| Date       | U-value [W/m <sup>2</sup> K] | n (valid minutes) | PCM state | $\bar{q}$ [W/m <sup>2</sup> ] | $\Delta T$ [K] |
|------------|------------------------------|-------------------|-----------|-------------------------------|----------------|
| 07/02/2023 | 0.248                        | 945               | Solid     | +1.64                         | -6.60          |
| 17/03/2023 | 0.593                        | 780               | Solid     | +4.82                         | -8.11          |
| 19/03/2023 | 0.498                        | 869               | Solid     | +3.29                         | -6.61          |
| 27/08/2023 | 0.289                        | 711               | Liquid    | +2.32                         | -8.01          |
| 23/10/2023 | 0.102                        | 895               | Solid     | +0.56                         | -5.48          |
| 25/10/2023 | 0.233                        | 935               | Solid     | +1.71                         | -7.32          |
| 29/10/2023 | 0.090                        | 969               | Solid     | +0.53                         | -5.91          |
| 25/07/2025 | 0.342                        | 507               | Liquid    | +1.37                         | -4.01          |
| 26/07/2025 | 0.534                        | 544               | Liquid    | +2.70                         | -5.05          |

These values represent the intrinsic thermal transmittance of the facade module when the PCM is fully solidified and functioning purely as a passive insulator.

### 3.7.4. Calculation of Energy-Comfort Performance Index

The ECPI was calculated for representative days (see Table 3.2) across winter, spring, summer and autumn under different operational regimes (fully Passive, fully Active and hybrid day/night switching). By applying the same calculation procedure to both the developed facade system and the reference system, the results provide a consistent basis for ranking performance across weather conditions and identifying which regimes yield the most favourable balance between indoor comfort stability and energy demand.

In Fig. 3.12, the calculated results are summarised and arranged in ascending order according to the ECPI values of the tested technology.

Based on the calculated ECPI values, it can be observed that the developed adaptive facade generally demonstrates lower overall performance when operating continuously in either fully Passive or fully Active modes. Two notable exceptions to this trend are identified. First, under moderate outdoor temperatures combined with moderate solar irradiance, the Passive mode yields competitive ECPI values. These conditions typically correspond to temperate summer periods, where solar gains are sufficient to support indoor stability without causing overheating, and auxiliary energy demand remains limited. Second, under low outdoor temperatures (approximately 0 °C) and reduced solar irradiance, the Active mode performs comparatively

well, reflecting conditions characteristic of mild winter periods, where controlled heat pump operation effectively stabilises indoor temperature without excessive electricity consumption.

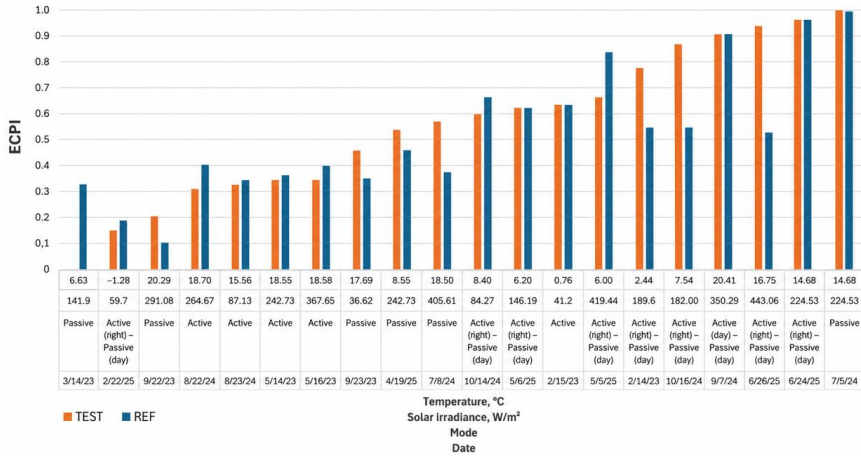


Fig. 3.12. Comparison of calculated ECPI values for solar facade and reference technologies.

The ECPI analysis further indicates that the most consistently favourable performance of the developed technology occurs in the Active (night) – Passive (day) regime during transitional seasons. In these mid-season conditions, nocturnal activation supports thermal stabilisation and pre-conditioning, while daytime passive operation enables effective utilisation of solar gains and stored thermal energy. Conversely, during hot and sunny summer conditions, the highest ECPI values are achieved under the Active (day) – Passive (night) regime. In this case, daytime active control mitigates overheating risk, while passive night operation benefits from reduced cooling demand and natural temperature decline.

After identifying regime-dependent performance patterns from the single-day ECPI analysis, extended five-day periods representing the most characteristic and energetically relevant operating modes were examined in greater detail. The selected five-day periods corresponding to the identified optimal regimes are summarised in Table 3.4.

Table 3.4

Five-day Periods for Detailed ECPI Calculation

| Mode                           | Season               | Dates         |
|--------------------------------|----------------------|---------------|
| Passive (day) – Active (night) | Spring/Autumn (cool) | 6–10/03/2025  |
| Passive (day) – Active (night) | Spring/Autumn (warm) | 9–13/05/2025  |
| Passive (night) – Active (day) | Summer (hot)         | 9–13/09/2024  |
| Passive                        | Summer (warm)        | 3–7/07/2024   |
| Active                         | Winter (medium)      | 15–19/02/2023 |

Figures 3.13 to 3.17 present the calculated ECPI values for the selected five-day periods representing the most characteristic operating regimes identified in the previous analysis.

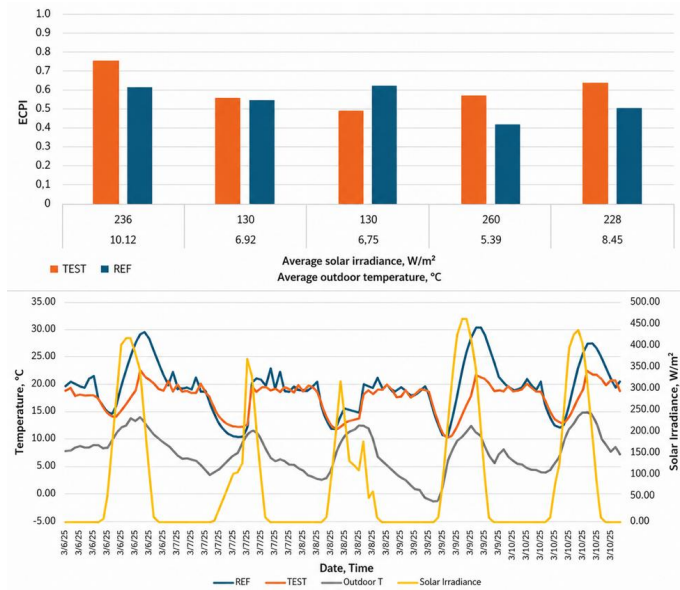


Fig. 3.13. Comparison of calculated ECPI values for a five-day period from 6–10/03/2025.

In the observed five-day period (cool mid-season), it is evident that only on the third day, the developed technology’s efficiency is lower compared to the reference (see Fig. 3.13). On this day, the lowest average outdoor temperature and solar irradiance are also observed. The overall average efficiency across the whole period is 6 % higher for the developed technology.

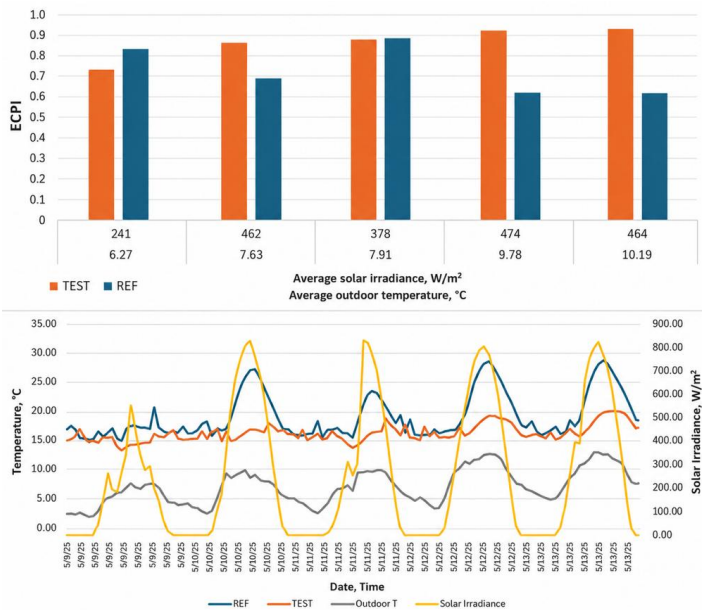


Fig. 3.14. Comparison of calculated ECPI values for a five-day period from 9–13/05/2025.

In a warm mid-season five-day period (see Fig. 3.14), a similar trend emerges: at lower average outdoor temperature and solar irradiance, the ECPI value of the developed technology is lower (day 1 and day 3). Comparing average ECPI across the whole period, it is 13 % higher for the solar facade.

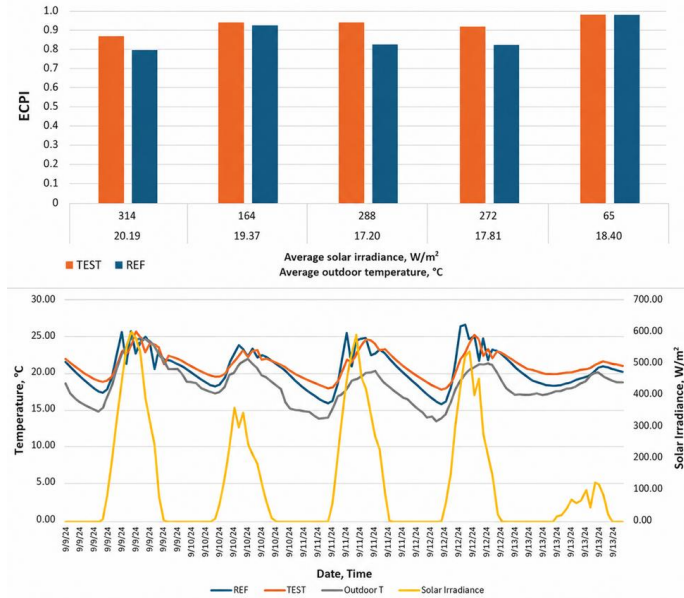


Fig. 3.15. Comparison of calculated ECPI values for a five-day period from 9–13/09/2024.

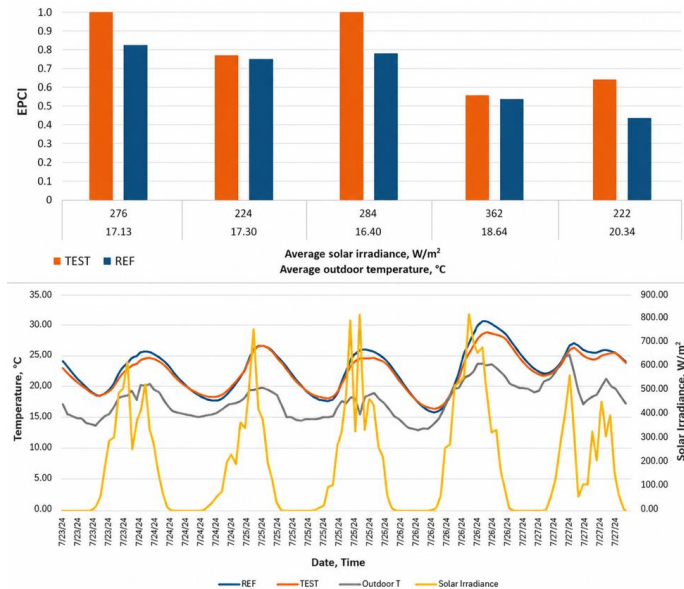


Fig. 3.16. Comparison of calculated ECPI values for a five-day period from 3–7/07/2024.

In the hot summer period with the Passive (night) – Active (day) regime (see Fig. 3.15), both technologies show high ECPI values (not lower than 0.8), while the solar facade performance is slightly higher or equal to the reference on all days. The average ECPI across the entire period is 6 % higher for the solar facade.

In warm summer conditions (Fig. 3.16), with the experimental stand operating fully in Passive mode, the solar facade shows higher EPCI than the reference stand on all days, reaching the maximum value on two days (day 1 and day 3). Overall, the value of EPCI in the period is 13 % higher for the developed technology.

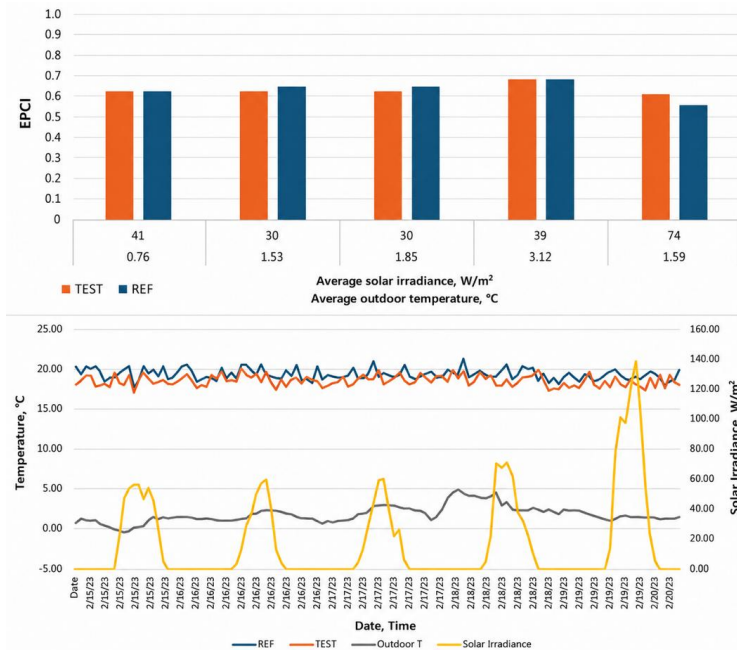


Fig. 3.17. Comparison of calculated ECPI values for a five-day period from 15–19/02/2023.

During the winter five-day period (15–19/02/2023) both stands were tested in Active mode (see Fig. 3.17). Both technologies show very similar EPCI values, leading to an equal overall balance. It can be observed how sensitive both technologies are to temperature fluctuations, which directly affect efficiency for both technologies across the period. On the final day, when slightly higher solar irradiance intensity is observed, the solar facade reflects this in a higher EPCI value.

### 3.7.5. Conclusions and insights (E7 – TEST A/P/H)

Over the course of two years, a wide range of experiments were carried out under varying seasonal and weather conditions to evaluate the effectiveness of different operational regimes and the impact of PCM integration on thermal performance and energy efficiency. One of the central findings of the study is that the effectiveness of the dynamic facade system is highly

dependent on the selected control regime and the prevailing weather conditions. Three main regimes were evaluated: Passive (day) – Active (night), Active (24/7) and fully Passive. Each of these regimes displayed specific strengths and limitations depending on the season.

The Passive (day) – Active (night) regime emerged as the most balanced and energy-efficient approach, particularly during the spring and autumn months. These transitional seasons offer moderate solar irradiance during the day and cooler temperatures at night – conditions under which the PCM could successfully undergo phase transitions. On sunny days, the PCM absorbed excess solar heat, preventing overheating in the test booth and released the stored heat during colder nighttime hours when the heat pump was reactivated. This led to improved indoor temperature stability and reduced energy consumption in many cases. On cloudy days in spring and autumn, the benefits of this regime were still apparent, although less pronounced. The PCM was occasionally able to reach its solidification point and release heat, offering limited thermal support. Notably, during such conditions, the energy consumption of the test stand was often slightly lower than that of the reference stand, suggesting that even under reduced solar input, the PCM contributed to thermal buffering.

In contrast, the Active regime, where heat pumps operated continuously to maintain target indoor temperatures, showed less distinction between the test and reference stands. In many instances, both booths maintained similar indoor temperatures with nearly identical energy consumption. However, during hot, sunny days in summer, the PCM in the test booth absorbed not only solar gains but also indoor heat from the heat pump, especially when it remained in a fully melted state. This led to a situation where the heat pump was effectively dissipating the very heat that the PCM was absorbing, creating an energy loop that reduced system efficiency. These findings highlight the importance of optimising the control algorithm to recognise when the PCM should be allowed to absorb heat and when it should be insulated to prevent unnecessary charging during active cooling phases.

The fully Passive regime was most beneficial during sunny summer days, particularly in avoiding indoor overheating. In several test cases, the reference booth experienced indoor temperatures exceeding 40 °C, while the test booth, protected by the PCM, remained significantly cooler – often not exceeding 36 °C. The PCM acted as an effective thermal barrier, absorbing excess heat and moderating the indoor environment. However, it is important to note that the PCM often remained above its melting point throughout the day and night, functioning primarily in its sensible heat range rather than undergoing a full phase transition. As a result, the system's energy storage potential was limited, even though comfort was improved.

During winter, the benefits of PCM integration were more constrained. Due to consistently low solar irradiance and low ambient temperatures, the PCM often failed to reach its melting point. Both the test and reference booths required active heating to maintain comfort, and in some cases, the test booth consumed slightly more energy due to the additional thermal mass and delayed temperature response associated with the PCM. However, on rare sunny winter days, the PCM was able to contribute marginally to thermal stability by capturing limited solar gains during the day and releasing some heat at night, although the overall impact on energy savings was modest.

The seasonal energy consumption data collected over 2023 and 2024 support these observations. In both years, consumption patterns of the test and reference booths varied by weather and regime, but in several key periods, particularly during the Passive (day) – Active (night) mode in spring and autumn, the test stand demonstrated either equal or slightly lower energy demand. In contrast, during fully active operation in summer, the test stand occasionally consumed more energy, especially when the PCM acted as a competing thermal sink during cooling.

The calculated U-values derived exclusively from periods without solar radiation provide a clear and consistent picture of the true conductive performance of the PCM-integrated solar facade module. When the PCM remained fully solid, and no solar charging occurred, the module exhibited very low thermal transmittance values – 0.09–0.25 W/m<sup>2</sup>K during the late-autumn and mid-winter days (23/10, 25/10, 29/10 and 07/02) – demonstrating insulation performance that significantly surpasses that of the reference triple-glazed window (U = 0.85 W/m<sup>2</sup>K) installed in the comparison booth. Even during the early spring days (17/03 and 19/03), when the module's U-value increased to 0.50–0.60 W/m<sup>2</sup>K, the facade still consistently outperformed the reference window by providing 30–50 % lower thermal transmittance. These seasonal differences reflect the temperature sensitivity of the PCM layer: the October and February values correspond to a fully solid PCM with maximal thermal resistance, while the higher March values arise from elevated ambient conditions and early pre-melting behaviour, which reduce effective resistance even though the PCM does not undergo full phase transition.

Further insight is provided by the three analysed summer cases – 27/08/2023, 25/07/2025 and 26/07/2025 – during which the PCM remained fully liquid throughout the day and night. Under no-sun conditions, the module exhibited moderate conductive transmittance on 27/08/2023 (U ≈ 0.29 W/m<sup>2</sup>K), consistent with the higher thermal conductivity of liquid PCM. The two late-July 2025 cases produced conductive transmittance values of U ≈ 0.34–0.54 W/m<sup>2</sup>K, which align closely with the expected behaviour of the facade in the fully liquid regime. These summer results confirm that the PCM facade continues to provide better insulation performance than the reference window even when the PCM is liquid, although its effective resistance decreases compared to the solid-state winter conditions as conductive pathways become more active within the melted material.

While regime-based and thermal transmittance analyses provide essential physical understanding, the introduction of the ECPI adds an important multi-criteria dimension to the evaluation. The ECPI integrates two equally weighted components: thermal comfort compliance (time within the 15–25 °C indoor temperature band) and normalised electricity consumption of the heat pump. The ECPI results quantitatively confirm the regime-dependent behaviour observed in the experimental analysis. Continuous fully Passive or fully Active operation generally yields lower overall performance scores. The most favourable and consistent ECPI values occur in hybrid regimes aligned with seasonal characteristics. During transitional seasons, the Active (night) – Passive (day) strategy produces the highest performance scores, confirming that daytime passive solar harvesting combined with controlled nighttime stabilisation optimally activates the PCM's thermal storage potential. In hot summer

conditions, the optimal regime shifts toward Active (day) – Passive (night), where active daytime cooling mitigates overheating while passive night operation benefits from natural temperature reduction. This seasonal inversion of the optimal control strategy represents one of the key scientific insights of the study.

Extended five-day ECPI evaluations reinforce these conclusions. In cool mid-season conditions, the developed solar facade achieved, on average, 6 % higher ECPI values than the reference system. In warm mid-season conditions, the advantage increased to 13 %. During hot summer operation under the hybrid regime, both systems performed strongly ( $ECPI > 0.8$ ), yet the solar facade maintained a consistent 6 % advantage. Under fully Passive warm summer conditions, the solar facade achieved a 13 % higher overall ECPI. In winter Active mode, both systems demonstrated nearly identical performance, reflecting the limited contribution of PCM under low solar availability.

Taken together, these findings demonstrate that the developed adaptive solar facade does not simply reduce energy demand or improve comfort in isolation. Rather, it enhances the balance between energy consumption and thermal stability when operated under seasonally optimised control strategies. The solar facade system performs as a highly effective passive insulator during cold conditions, provides adaptive solar buffering during transitional periods, and significantly mitigates overheating in summer. Its full performance potential, however, is unlocked only when the operational regime is dynamically adjusted in accordance with climatic conditions.

## CONCLUSIONS

The main goal of this Thesis was to develop an innovative adaptive facade system integrating thermal energy storage through PCMs and to evaluate its effectiveness in enhancing building energy performance under both controlled laboratory and real outdoor conditions.

The research was motivated by the urgent need to improve the energy performance of the European building stock in alignment with the European Green Deal, the EPBD and the Renovation Wave Strategy. Buildings remain one of the largest consumers of final energy and sources of CO<sub>2</sub> emissions within the European Union. Consequently, innovation at the building-envelope level represents a critical pathway toward achieving long-term climate neutrality objectives. The present work addresses this challenge by combining material-level analysis, small- and large-scale experimentation and numerical modelling within a structured methodological framework.

The literature review established the scientific, technological and policy foundations of the research. It confirmed that LHTES, particularly through solid-liquid PCMs, offers significantly higher storage density than sensible heat systems and enables energy exchange at nearly constant temperatures. This characteristic makes PCMs especially suitable for integration into building envelopes, where they can moderate indoor temperature fluctuations, reduce peak loads and enhance solar energy utilisation. The review also highlighted that, despite extensive laboratory investigations, long-term full-scale validation of PCM-integrated adaptive facades remains limited. Furthermore, it emphasised that steady-state U-value measurements alone are insufficient to characterise dynamic solar facades; instead, real-climate experimental evaluation combined with transient simulation is required. These identified gaps directly shaped the experimental and modelling strategy adopted in this Thesis.

The testing of properties for RT21HC and RT28HC PCMs provided essential thermophysical input parameters for facade development. Repeated guarded hot-plate experiments across twelve rounds confirmed stable and repeatable thermal conductivity values of 0.255 W/(m·K) for RT21HC and 0.30 W/(m·K) for RT28HC. Although certain rounds were influenced by imperfect boundary control, particularly limited cooling performance, the overall dataset demonstrated sufficient consistency to support numerical modelling. RT21HC exhibited more stable thermal behaviour during heating and cooling cycles, while RT28HC showed slightly greater sensitivity to boundary conditions. Comparative steady-state and dynamic testing further revealed that, under Northern European climatic conditions, RT21HC provided more favourable thermal contributions to indoor air temperature despite RT28HC occasionally reaching higher peak PCM temperatures. This indicates that RT21HC more effectively utilised latent heat storage in transitional climates, whereas RT28HC displayed a stronger sensible heat response when complete melting was not achieved.

The validated S1 numerical model successfully reproduced the dominant phase-change dynamics observed experimentally, particularly under moderate boundary conditions. Good agreement between simulated and measured temperatures confirmed the physical reliability of the adopted material parameters and modelling approach. Deviations under extreme heating or cooling conditions were primarily attributed to experimental boundary inconsistencies rather

than modelling deficiencies. This validated framework enabled further development of the small-scale simulation model (S2) under realistic climatic boundary conditions, demonstrating that RT21HC is a more suitable option for the development of an adaptive solar facade in colder climates.

Small-scale laboratory and outdoor experiments demonstrated that facade performance is highly sensitive to insulation configuration and optical–thermal interaction. The introduction of adjustable insulation layers increased both PCM and indoor temperatures across all setups, with the most pronounced improvements observed in configurations including an air-gap layer. These modules exhibited slower heat dissipation during the discharge phase, indicating improved thermal retention. When evaluating the complete charging–discharging cycle, air-gap configurations gained and released more energy overall, whereas more heavily insulated setups demonstrated greater stability during latent heat plateaus.

The integration of dynamic components – reflective blades combined with aerogel insulation and a Fresnel lens – produced measurable performance enhancements. Under laboratory conditions, the dynamic configuration improved PCM charging rates and extended effective discharge periods. Outdoor validation confirmed that dynamic blade actuation enhanced late-day solar capture, particularly as solar azimuth angles shifted. Systematic focal-point optimisation revealed that both cone diameter and focal position significantly influence heat-transfer efficiency. Setup F1 D4 achieved the highest balanced performance, reaching a maximum daytime PCM temperature of 19.52 °C while maintaining favourable end-of-cycle retention. These findings demonstrate that geometric precision and component synergy are critical to overall facade efficiency.

The two-year large-scale PASLINK-type experimental testing provided comprehensive insight into seasonal and regime-dependent behaviour. The results clearly show that facade performance is strongly influenced by the selected operational regime and prevailing climatic conditions. During spring and autumn, the Passive (day) – Active (night) regime delivered the most balanced and energy-efficient performance. Under these conditions, daytime solar gains enabled partial or full PCM charging, while nighttime discharge supported indoor thermal stability and often reduced heat pump demand. Even during partially cloudy transitional periods, modest buffering effects were observed.

In summer, fully Passive operation proved particularly beneficial for overheating mitigation. The reference booth frequently exceeded indoor temperatures of 40 °C, whereas the PCM-integrated test booth typically remained below 36 °C. Although the PCM often operated within its sensible heat range rather than completing full phase transitions, it nonetheless acted as an effective thermal buffer. Conversely, under fully Active summer operation, inefficiencies emerged when the PCM absorbed heat that was simultaneously being removed by the cooling system, creating counterproductive thermal loops.

Winter results demonstrated limited PCM activation due to low solar irradiance and ambient temperatures. However, the facade exhibited excellent insulation performance. Under no-solar conditions with fully solid PCM, the module achieved U-values between 0.09 W/m<sup>2</sup>K and 0.25 W/m<sup>2</sup>K during late autumn and mid-winter periods, substantially outperforming the reference triple-glazed window (U = 0.85 W/m<sup>2</sup>K). Even in early spring, when U-values

increased to 0.50–0.60 W/m<sup>2</sup>K due to partial pre-melting, the facade still maintained 30–50 % lower thermal transmittance than the reference. In fully liquid summer states, U-values ranged from approximately 0.29 W/m<sup>2</sup>K to 0.54 W/m<sup>2</sup>K, remaining superior to the reference system. These findings confirm that the facade provides year-round insulation advantages independent of phase-change activation.

The ECPI, combining thermal comfort compliance and normalised heat pump electricity consumption, provided an integrated performance metric. ECPI results quantitatively confirmed the regime-dependent behaviour observed experimentally. Hybrid seasonal strategies consistently produced the highest performance scores. In cool mid-season periods, the adaptive facade achieved approximately 6 % higher ECPI values than the reference system, while in warm mid-season conditions, the advantage increased to 13 %. During hot summer hybrid operation, both systems achieved high ECPI values (above 0.8), yet the adaptive facade maintained a 6 % advantage. Under fully Passive warm summer conditions, the advantage reached 13 %. In winter Active mode, both systems performed nearly identically, reflecting limited PCM contribution under low solar availability.

Taken together, these results demonstrate that the adaptive PCM-integrated solar facade does not universally reduce energy demand under all conditions. Rather, it enhances the balance between energy consumption and thermal stability when operated under seasonally optimised regimes. The hypothesis of the Dissertation is therefore partially confirmed. PCM integration demonstrably improves thermal performance, overheating mitigation and energy efficiency under suitable climatic and operational conditions. However, its effectiveness depends strongly on solar availability, control strategy, and coordination of heat pumps.

The research makes several key contributions. It provides long-term, full-scale validation of a PCM-integrated adaptive solar facade under Northern European conditions. It establishes a multi-scale methodological framework linking material characterisation, small-scale optimisation, dynamic outdoor testing and performance-index evaluation. It demonstrates the insulation superiority of PCM-enhanced facades and identifies regime-specific optimisation strategies. Finally, it proposes practical improvements including heat-exchanger integration, nanoparticle-enhanced PCM formulations and advanced predictive control algorithms.

In conclusion, this Thesis demonstrates that adaptive solar facades integrating PCMs represent a technically viable and scientifically validated approach to improving building-envelope performance. Their effectiveness is maximised through seasonally adaptive control strategies and integrated system design. By combining thermal storage, optical concentration, high-performance insulation and dynamic operation, the developed facade concept contributes meaningfully to advancing energy-efficient and climate-responsive building technologies aligned with European decarbonisation goals.

## REFERENCES

- [1] European Commission, The European Green Deal, European Commission – Press Re 53 (2019) 24. <https://doi.org/10.1017/CBO9781107415324.004>.
- [2] European Commission, Clean energy for all Europeans, Euroheat and Power 14 (2019) 3. <https://doi.org/10.2833/9937>.
- [3] EU, Directive (EU) 2018/844 of the European Parliament and of the Council amending Directive 2010/31/EU on the energy performance of buildings and Directive 2012/27/EU on energy efficiency, 2018.
- [4] EU, Directive (EU) 2018/2001 of the European Parliament and of the Council on the promotion of the use of energy from renewable sources, Official Journal of the European Union 2018 (2018) 82–209.
- [5] M. Lazzaroni, G. Bianchi Porro, Preparation, premedication and surveillance, *Endoscopy* 35 (2003) 103–111. <https://doi.org/10.1055/s-2003-37012>.
- [6] M. Economidou, V. Todeschi, P. Bertoldi, D. D’Agostino, P. Zangheri, L. Castellazzi, Review of 50 years of EU energy efficiency policies for buildings, *Energy Build.* 225 (2020) 110322. <https://doi.org/10.1016/j.enbuild.2020.110322>.
- [7] D. Kumar, M. Alam, P. X. W. Zou, J. G. Sanjayan, R. A. Memon, Comparative analysis of building insulation material properties and performance, *Renewable and Sustainable Energy Reviews* 131 (2020) 110038. <https://doi.org/10.1016/j.rser.2020.110038>.
- [8] B. Nashaat, A. Waseef, Responsive Kinetic Facades: An Effective Solution for Enhancing Indoor Environmental Quality in Buildings RESPONSIVE KINETIC FACADES : AN EFFECTIVE SOLUTION, (2017) 0–13.
- [9] Directive (EU) 2018/844 of the European Parliament and of the Council, Official Journal of the European Union L156 (2018).



**Jānis Narbutis** was born in 1987 in Riga. He obtained a Professional Bachelor's degree in Electrical Engineering (2010), a Professional Master's degree in Computerised Control of Electrical Technologies (2011), and a Master's degree in Environmental Science (2021) from Riga Technical University (RTU). Since 2022, he has been a Researcher at the RTU Institute of Energy Systems and Environment. During his studies, he participated in the Erasmus exchange programme at the Polytechnic University of Turin (Italy). He is the author of several scientific publications on adaptive facades, phase change materials and building energy efficiency. His scientific interests are related to adaptive building envelopes, thermal energy storage and sustainable energy technologies.